In situ cleaning of metal cathodes using a hydrogen ion beam

D. H. Dowell,* F. K. King, R. E. Kirby, and J. F. Schmerge
SLAC, Menlo Park, California 94025, USA

J. M. Smedley
BNL, Upton, New York, USA
(Received 29 March 2006; published 22 June 2006)

Metal photocathodes are commonly used in high-field rf guns because they are robust, straightforward to implement, and tolerate relatively poor vacuum compared to semiconductor cathodes. However, these cathodes have low quantum efficiency (QE) even at UV wavelengths, and still require some form of cleaning after installation in the gun. A commonly used process for improving the QE is laser cleaning. In this technique the UV-drive laser is focused to a small diameter close to the metal's damage threshold and then moved across the surface to remove contaminants. This method does improve the QE, but can produce nonuniform emission and potentially damage the cathode. Ideally, an alternative process which produces an atomically clean, but unaltered, surface is needed. In this paper we explore using a hydrogen ion (H-ion) beam to clean a copper cathode. We describe QE measurements over the wavelength range of interest as a function of integrated exposure to an H-ion beam. We also describe the data analysis to obtain the work function and derive a formula of the QE for metal cathodes. Our measured work function for the cleaned sample is in good agreement with published values, and the theoretical QE as a function of photon wavelength is in excellent agreement with the cleaned copper experimental results. Finally, we propose an *in situ* installation of an H-ion gun compatible with existing s-band rf guns.

DOI: 10.1103/PhysRevSTAB.9.063502 PACS numbers: 07.77.Ka, 52.59.−f, 71.10.Ca, 85.60.Ha

I. INTRODUCTION AND DESCRIPTION OF THE EXPERIMENT

Improving and maintaining the quantum efficiency (QE) of a metal photocathode in an s-band rf gun requires a process for cleaning the surface. In this type of gun, the cathode is typically installed and the system is vacuum baked to ~200 °C. If the QE is too low, the cathode is usually cleaned with the UV-drive laser. While laser cleaning does increase the cathode QE, it requires fluences close to the damage threshold and rastering the small diameter beam, both of which can produce nonuniform electron emission and potentially damage the cathode.

This paper investigates the efficacy of using a low-energy hydrogen ion beam to produce high-QE metal cathodes. Measurements of the QE vs wavelength, surface contaminants using x-ray photoelectron spectroscopy, and surface roughness were performed on a copper sample, and the results showed a significant increase in QE after cleaning with a 1 keV hydrogen ion beam. The H-ion beam cleaned an area approximately 1 cm in diameter and had no effect on the surface roughness while significantly increasing the QE. The work function for copper is extracted from this data. In addition, a formula of the QE for metals as a function of optical wavelength is derived assuming the 3-step process for photoemission and using the Fermi-Dirac distribution for the electron density of states (EDOS). The theory is in excellent agreement with measurements of QE for a clean copper surface. These results and a method for installing an H-ion cleaner on existing s-band guns are described.

A. Sample preparation and surface roughness

A sample of oxygen-free, high conductivity copper 25 mm in diameter and 2.5 mm thick was polished using 0.25 μm diamond paste in a standard procedure for cathodes which are used in rf guns. After polishing the sample was stored under hexane, which over time had evaporated, resulting in an oxidized carbon surface and a very low initial QE (Fig. 2). It is this sample upon which the QE studies described below were performed.

A second sample was used to study the surface roughness and determine if there was any change in the surface morphology due to the exposure to the H-ion beam. This is important in high-field rf guns since any roughening of the surface will produce undesirable dark current. Atomic force microscope (AFM) measurements on this similarly polished and H-ion treated second sample gave the following results [1]. The Ra and Rq before treatment were 10.55 and 13.09 nm, respectively, and the peak-to-peak roughness was 187.91 nm. After exposure to H-ions the respective values were 12.48, 15.65, and 118.76 nm for one 50×50 μm area and 10.19, 12.52, and 82.50 nm for another 50×50 μm area. Two areas were measured in order to estimate the systematic uncertainly of not being able to reposition the probe in exactly the same region on the sample when removed and then reinstalled in the AFM.

*To whom correspondence should be addressed.
Electronic address: dowell@slac.stanford.edu

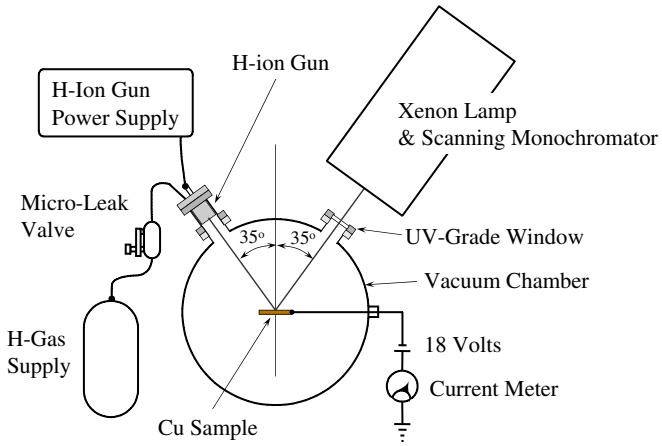

FIG. 1. (Color) Schematic of the experimental configuration used to measure the QE as a function of wavelength and to clean the sample. The 18 V battery is not in the circuit when measuring the H-ion gun current during cleaning.

B. QE and surface contamination measurements

After preparation, the sample was placed in a load lock chamber separated by a valve from an x-ray photoelectron spectroscopy (XPS) measurement chamber. The XPS data provided the percentage coverage of carbon on the surface. The QE measurements and the H-ion cleaning were performed in the load lock chamber with the geometry shown in Fig. 1. The QE was determined with the sample biased at -18 V relative to the surrounding chamber. This was done to ensure that no secondary electrons generated by the chamber walls could return to the sample. Since there was a large gap (of order centimeters) to the nearest ground, the electric field on the sample was essentially zero. The sample was illuminated by light from a xenon arc lamp whose output was selected by a scanning monochromator with a slit set to pass a wavelength range of 8 nm. The transmission of the vacuum window and other optics were measured and used to determine the absolute QE. The H-ion beam was produced by a commercial saddle field ion source [2], whose beam energy was approximately 1 keV. Ion currents of 0.4, 0.7, and 2 μA were used. Labview [3] software automatically scanned the wavelength in 2 nm steps while collecting the photocurrents and background currents. The experiment determined the QE and the surface contamination as the sample was progressively exposed to the H-ion beam.

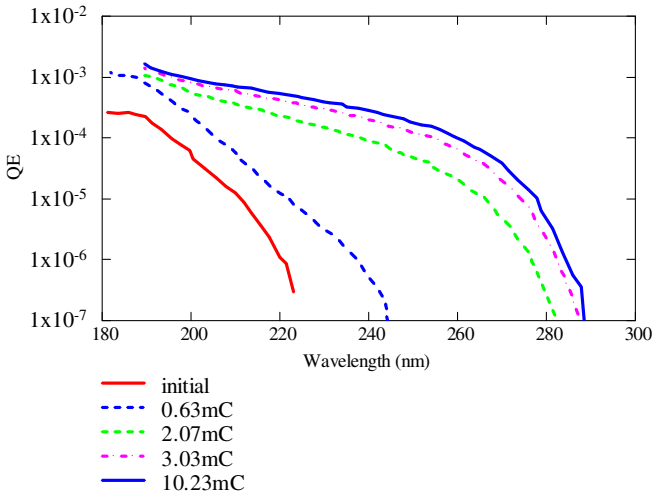

FIG. 2. (Color) The QE for a copper sample vs wavelength with increasing integrated exposure to the H-ion beam.

The data for the unbaked copper sample are shown in Fig. 2. In other experiments it is standard practice to bake the sample to 230 °C to clean the surface. In this case, however, we were interested in the effects of H-ion cleaning only; therefore the initial bake was not performed. The H-ion charge is measured by integrating the sample current, which may include a contribution from charged contaminants leaving the surface.

The results are quite dramatic, especially at the drive laser wavelengths of interest at 255 and 263 nm. Although the sample was exposed to a total integrated H-ion charge of 10.23 milli-Coulomb (mC), most of the benefit was achieved by 3.03 mC. It should be noted that 250 μJ at 255 nm requires a QE of 2×10^{-5} to produce 1 nano-Coulomb of electrons.

II. DATA ANALYSIS

The QE data were analyzed to obtain the work function using the method of Fowler [4]. This technique includes the effect of temperature at photoemission threshold by assuming a Fermi distribution for the electrons and comparing the data with the following function:

$$\ln\left(\frac{QE}{T^2}\right) = B + \ln\left[f\left(\frac{\hbar\omega - \phi}{k_B T}\right)\right], \tag{1}$$

where T is the electron temperature (assumed to be 300 K), k_B is Boltzmann's constant, $\hbar\omega$ is the photon energy, and ϕ is the work function. B is a constant related to the electron density of states, the optical reflectivity, and electron transport to the surface. The function $f(x)$ results from integrals of the Fermi-Dirac function and is approximated by

$$f(x) = e^x - \frac{e^{2x}}{4} + \frac{e^{3x}}{9} - \cdots \qquad \text{for } x \le 0, \tag{2}$$

$$f(x) = \frac{\pi^2}{6} + \frac{x^2}{2} - \left(e^{-x} - \frac{e^{-2x}}{4} + \frac{e^{-3x}}{9} - \cdots\right) \tag{3}$$

for $x \ge 0$.

Fowler showed that ϕ and B are easily obtained by plotting the experimental $\ln(QE/T^2)$ vs the photon energy normalized to $k_B T$, and fitting with $B + \ln[f(\hbar\omega - \phi)/k_B T]$. Fowler plots are given for our six QE data sets in Figs. 3–5 and the percentage of carbon coverage is listed in the caption. The comparison with Fowler's theory is excellent with the exception of few cases. Figure 3 shows

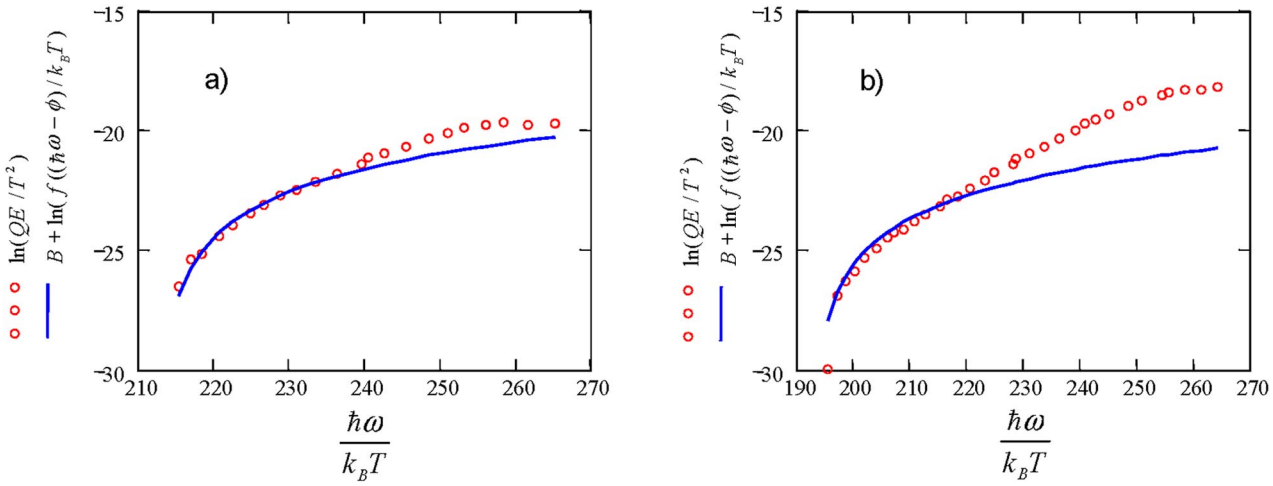

FIG. 3. (Color) Fowler plots for (a) the initial sample with 31% carbon surface coverage and (b) the same sample after exposure to 0.63 mC of H-ion beam has 11% carbon surface coverage.

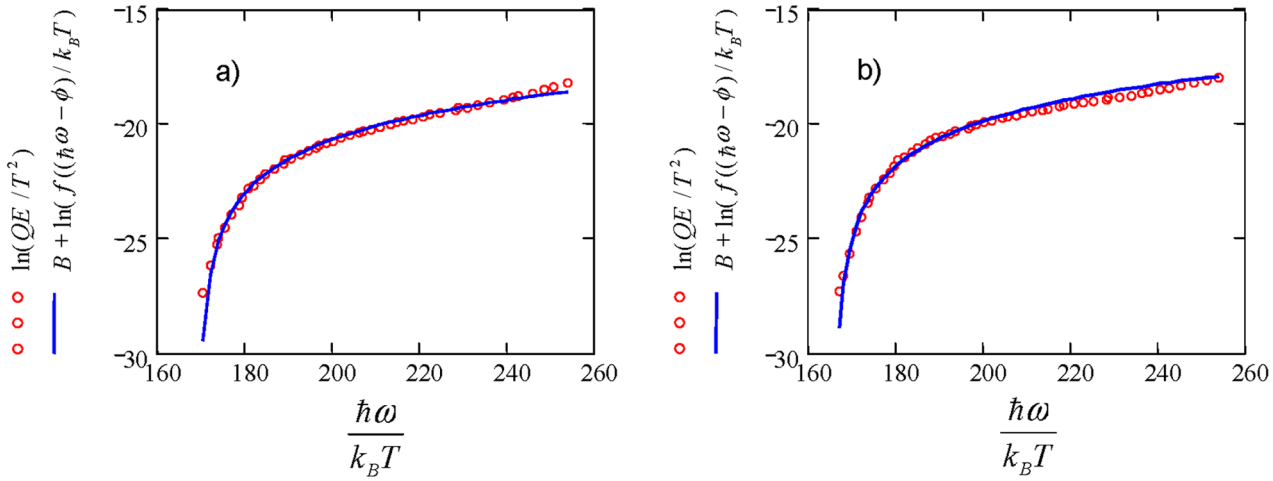

FIG. 4. (Color) Fowler plots for sample exposed to (a) 2.1 mC of H-ions with 12% carbon coverage and (b) after 3.0 mC of H-ions the carbon coverage is 10%.

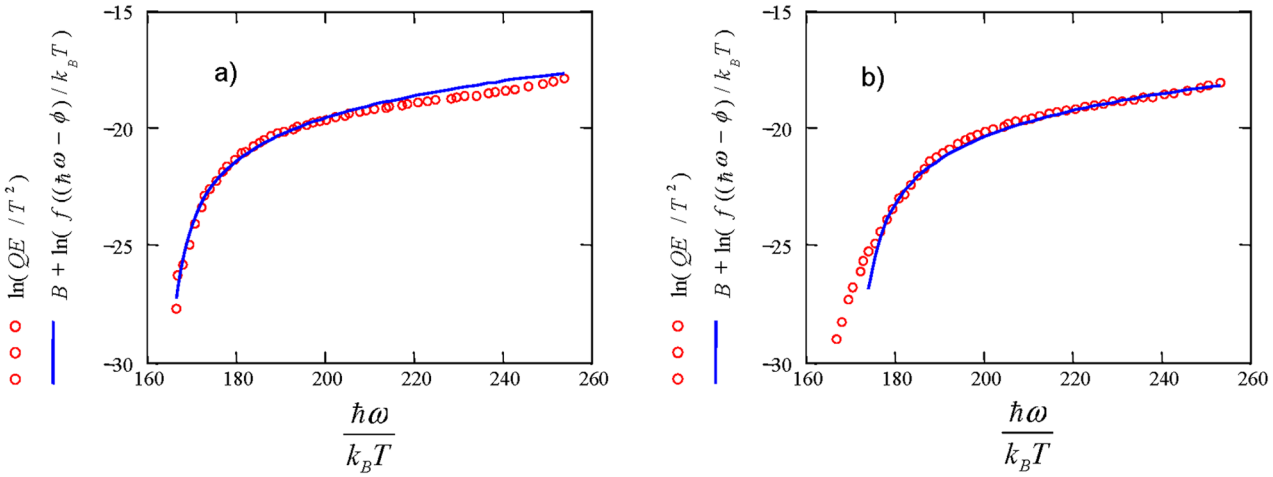

FIG. 5. (Color) (a) Fowler plot after final integrated exposure of 10.23 mC with a carbon coverage of 7%. (b) The result after heating the sample to 230 °C leaving a carbon coverage of 8%.

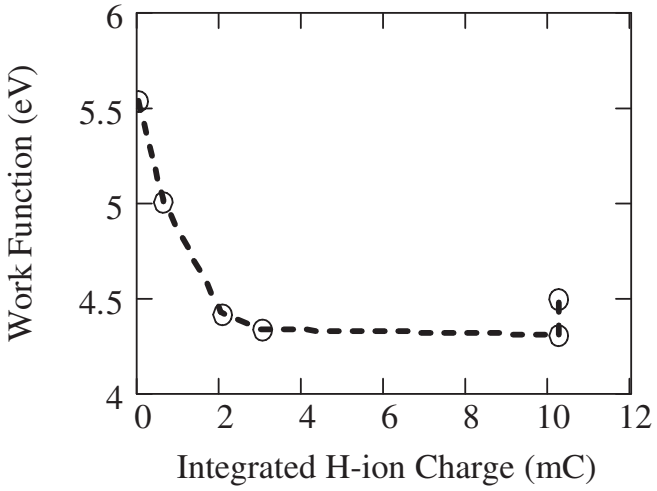

FIG. 6. The copper sample work function vs the accumulated H-ion charge. The higher work function point at 10.23 mC was measured after baking the H-ion cleaned sample to 230 °C.

the data and theory for the initial, contaminated sample with 31% carbon coverage and after a short exposure to the H-ion beam (0.630 mC). In these cases the fit has been biased to better match the threshold region. We assume the discrepancy at higher photon energies results from additional electron states not accounted for by the Fermi-Dirac distribution.

Another discrepancy is seen at low photon energies in Fig. 5(b) after 10.23 mC of H-ions and then heating the sample to 230 °C for 1 h. The bake was expected to further improve the QE, but instead the QE went down and the work function increased 0.18 eV. The data was fit with the Fowler function for values of $\hbar\omega/k_BT$ greater than 180, and best represents the data in both the threshold and higher photon energy regions. The contribution coming from the low-energy tail below 180 is a small and unexplained effect of the bake. As for the slight reduction (0.18 eV) in QE, we speculate this bake recontaminated the cathode either from outgassing of the surrounding adjacent chamber walls (only the sample was heated to 230 °C) or by diffusion of material from the sample's interior. However, it should be noted that previous measurements showed heating a contaminated sample to 230 °C in a clean UHV system resulted in QE's similar to those obtained with H-ion cleaning [1].

The work functions obtained for the copper sample as it was progressively cleaned by the H-ion beam are shown in Fig. 6. The final work function was 4.31 eV with an estimated systematic uncertainly of 0.2 eV. There was an increase of 0.18 eV when the sample was baked at 230 °C as described above.

Comparison with an accepted work function for polycrystalline copper is difficult because of the large range quoted in the literature. Therefore an average work function was computed with a standard deviation based upon the reported values [5–8]. The resulting work function is 4.66 ± 0.51 eV. Thus our value of 4.31 eV is in reasonable agreement.

III. DERIVATION OF THE QUANTUM EFFICIENCY FOR A METAL

In previous work [9], the QE was computed using the free-electron gas model of a metal and the Fermi-Dirac distribution for the EDOS [10]. This derivation of QE assumes the electrons are at zero temperature and imposes the requirement that the escaping electron's momentum perpendicular to the surface, $p_\perp$, satisfy [11]

$$\frac{p_\perp^2}{2m} > E_F + \phi - \phi_{\text{Schottky}}, \tag{4}$$

where ϕ is the work function, E_F the Fermi energy, and ϕ_{Schottky} is the barrier energy shift due to the Schottky effect which is conveniently expressed as $\phi_{\text{Schottky}} = 3.7947 \times 10^{-5}\sqrt{E(V/m)}$ eV [12]. For use in the following discussion, we define the effective work function, $\phi_{\text{eff}} = \phi - \phi_{\text{Schottky}}$.

Our calculation of the QE is based upon the three-step model for photoemission [13]. In this model, the electron is emitted by means of three sequentially independent processes: (i) absorption of the photon with energy $\hbar\omega$, (ii) migration including e-e scattering to the surface, and (iii) escape for electrons with kinematics above the barrier. Therefore the QE can be expressed in terms of the probabilities for these steps to occur:

$$QE(\omega) = [1 - R(\omega)]\frac{\int_{E_F+\phi_{\text{eff}}-\hbar\omega}^{\infty} dEN(E+\hbar\omega)[1 - f_{\text{FD}}(E+\hbar\omega)]N(E)f_{\text{FD}}(E)\int_{\cos\theta_{\max}(E)}^{1} d(\cos\theta)F_{\text{e-e}}(E,\omega,\theta)\int_0^{2\pi} d\Phi}{\int_{E_F-\hbar\omega}^{\infty} dEN(E+\hbar\omega)[1 - f_{\text{FD}}(E+\hbar\omega)]N(E)f_{\text{FD}}(E)\int_{-1}^{1} d(\cos\theta)\int_0^{2\pi} d\Phi}. \tag{5}$$

In the first step, a photon is absorbed by a metal with an optical reflectivity of $R(\omega)$ with a probability of $[1 - R(\omega)]$. $F_{\text{e-e}}$ is the probability that an electron reaches the surface without scattering with another electron. In the near-threshold regime we are concerned with, an electron-electron scattering event is not likely to result in either participating electron retaining energy sufficient to escape the material. Third is the probability that an electron will be excited by the photon into a state with sufficient perpendicular momentum to escape the material. Here we follow the method of Bergund and Spicer [10] in assuming that the probability of excitation of an electron with initial

energy E to final energy $E + \hbar\omega$ is solely a function of the number of filled states at energy E, $N(E)f_{\mathrm{FD}}(E)$, and the number of empty states at energy $E + \hbar\omega$, $N(E + \hbar\omega) \times [1 - f_{\mathrm{FD}}(E + \hbar\omega)]$. Here $f_{\mathrm{FD}}(E)$ refers to the Fermi-Dirac distribution function,

$$f_{\mathrm{FD}}(E) = \frac{1}{1 + e^{(E-E_F)/k_BT}}. \tag{6}$$

$N(E)$ refers to the number of electron states at energy E, often referred to as the EDOS. Implicit in this treatment is the assumption that there are no strong selection rules on the momentum states of the electron and that the quantum mechanical matrix element connecting the initial and final electron states is not itself a function of the electron energy. The maximum angle, $\theta_{\max}(E)$, at which an electron can approach the surface and still escape is determined by Eq. (4). The denominator in Eq. (5) is a normalizing factor that stems from the assumption that every photon that is not reflected leads to an excited electron.

Given that our goal is understanding near-threshold emission from copper, several assumptions can be made to simplify Eq. (5). First, the EDOS for copper is relatively flat from ~2 eV below the Fermi level to the vacuum level [12]. This allows us to assume $N(E)$ and $N(E + \hbar\omega)$ are constant. We assume that the Fermi-Dirac distribution can be taken at $T = 0$, resulting in steplike distribution with filled states up to E_F and empty states above E_F. For the near-threshold case considered here, $\theta_{\max}(E)$ will be near normal. This allows us to ignore the dependence of $F_{\text{e-e}}$ on the exact electron trajectory, and consider it a function of only the photon absorption depth and the electron mean-free path for a given photon energy $\hbar\omega$. Below we further simplify the scattering term by taking an average mean-free path for the electrons generated by a given photon energy. With these assumptions, Eq. (5) can be separated into three factors corresponding to the three-step process,

$$QE(\omega) = [1 - R(\omega)]F_{\text{e-e}}(\omega)\frac{\int_{E_F+\phi_{\mathrm{eff}}-\hbar\omega}^{E_F} dE \int_{\sqrt{(E_f+\phi_{\mathrm{eff}})/(E+\hbar\omega)}}^{1} d(\cos\theta) \int_0^{2\pi} d\Phi}{\int_{E_F-\hbar\omega}^{E_F} dE \int_{-1}^{1} d(\cos\theta) \int_0^{2\pi} d\Phi}. \tag{7}$$

These integrals are easily performed to give [9]

$$QE(\omega) = [1 - R(\omega)]F_{\text{e-e}}(\omega)\frac{(E_F + \hbar\omega)}{2\hbar\omega} \times \left[1 + \frac{E_F + \phi_{\mathrm{eff}}}{E_F + \hbar\omega} - 2\sqrt{\frac{E_F + \phi_{\mathrm{eff}}}{E_F + \hbar\omega}}\right]. \tag{8}$$

The electron-electron scattering term $F_{\text{e-e}}$ is derived using the distribution of excited electrons and the electron mean-free path due to e-e scattering, after the photon is absorbed into the metal to an optical skin depth λ_{opt}. Once the photon is absorbed, the excited electrons drift to the metal's surface with some scattering against the valence electrons and losing enough energy to remain bound. The e-e scattering length $\lambda_{\text{e-e}}$ or electron mean-free path between collisions with valence electrons determines how many excited electrons reach the surface without any collision. We assume that any collision eliminates the electron's chance to escape. Therefore, the fraction of electrons per unit distance which avoid scattering at a distance s from the surface is given by

$$f(s) = \frac{1}{\lambda_{\mathrm{opt}}} e^{-s[(1/\lambda_{\mathrm{opt}})+(1/\lambda_{\text{e-e}})]}. \tag{9}$$

Integrating into the metal several skin depths gives the fraction of electrons reaching the surface,

$$F_{\text{e-e}} = \int_0^{\infty} f(s)ds = \frac{1}{1 + \frac{\lambda_{\mathrm{opt}}}{\lambda_{\text{e-e}}}}, \tag{10}$$

and the expression for the QE then becomes

$$QE(\omega) = \frac{1 - R(\omega)}{1 + \frac{\lambda_{\mathrm{opt}}}{\lambda_{\text{e-e}}}} \frac{E_F + \hbar\omega}{2\hbar\omega} \times \left[1 + \frac{E_F + \phi_{\mathrm{eff}}}{E_F + \hbar\omega} - 2\sqrt{\frac{E_F + \phi_{\mathrm{eff}}}{E_F + \hbar\omega}}\right]. \tag{11}$$

The optical skin depth depends upon wavelength and is given by $\lambda_{\mathrm{opt}} = \frac{\lambda}{4\pi k}$, where k is the imaginary part of the complex index of refraction, $\eta = n + ik$, and λ is the free space photon wavelength.

The electron-electron scattering length is energy dependent and can be derived from the Pauli exclusion principle, which constrains the final state energies of both the valance and excited electrons to above the Fermi level. Here we solve for the energy dependence of the e-e scattering length assuming the excited electron scatters only with valence electrons (electrons below the Fermi level) and any scattering event eliminates the electron from escaping. The probability for e-e scattering of an electron with energy E is proportional to the number of occupied initial and unoccupied final electron states for a valence electron with energy E_0, as well as the availability of vacant states at $E_0 + \Delta E$ and $E_0 - \Delta E$, for the final valence and excited electron states,

$$P(E, E_0, \Delta E) \propto N(E_0)f_{\mathrm{FD}}(E_0)N(E_0 + \Delta E) \times [1 - f_{\mathrm{FD}}(E_0 + \Delta E)]N(E - \Delta E) \times [1 - f_{\mathrm{FD}}(E - \Delta E)]. \tag{12}$$

As above, we assume that the EDOS is constant, and

evaluate the Fermi-Dirac functions at $T = 0$. The probability can then be written in terms of Heaviside-step functions, $H(x)$ [14],

$$P(E, E_0, \Delta E) \propto H(E_F - E_0)H(E_0 + \Delta E - E_F) \times H(E - E_0 - 2\Delta E). \quad (13)$$

The first factor on the right expresses that the valence electron's initial energy must be less than the Fermi energy, $E_0 < E_F$, the second step function requires that the energy gained by the valence electron from scattering with the excited electron must increase the valence electron's energy over the Fermi level, $E_0 + \Delta E > E_F$, and the third factor only allows scattering of the valence electrons to unoccupied states with energies less than the excited electrons final energy level, $E - E_0 < 2\Delta E$. This prevents double counting cases where the valence electron ends up with higher energy than the excited electron due to the indistinguishable nature of electrons. Therefore the energy exchanged is bounded, $E_F - E_0 < \Delta E < (E - E_0)/2$ and the initial valence electron energy constrained to $2E_F - E < E_0 < E_F$.

The total probability an electron with energy E scatters is then given by

$$P(E) = \int dE_0 \int d(\Delta E) P(E, E_0, \Delta E) \propto \int_{2E_F - E}^{E_F} dE_0 \int_{E_F - E_0}^{(E-E_0)/2} d(\Delta E). \quad (14)$$

Performing these trivial integrals gives

$$P(E) \propto \tfrac{1}{4}(E - E_F)^2. \quad (15)$$

The electron scattering length, $\lambda_{\text{e-e}}$, is found by using Fermi's golden rule [15] which relates the transition rate $\tau(E)$, to the electron velocity $\nu(E)$ and the inverse of the transition probability $P(E)$ [12],

$$\lambda_{\text{e-e}}(E') = \nu(E')\tau(E') \propto \frac{\nu(E')}{P(E')} \propto \frac{1}{E'^{3/2}}. \quad (16)$$

Following the discussion and derivation given in Ref. [16], we assume the energy for the electron in the conduction band is relative to the Fermi level and compute its velocity, $\nu(E - E_F) = \sqrt{2(E - E_F)/m}$, and define $E' = E - E_F$. Normalizing the scattering length to a known value at energy E_m above the Fermi level gives the energy dependent electron scattering length,

$$\lambda_{\text{e-e}}(E') = \lambda_{\text{e-e}}(E_m)\left(\frac{E_m}{E'}\right)^{3/2}. \quad (17)$$

This result is plotted in Fig. 7, illustrating the energy dependence of the e-e scattering length. This expression

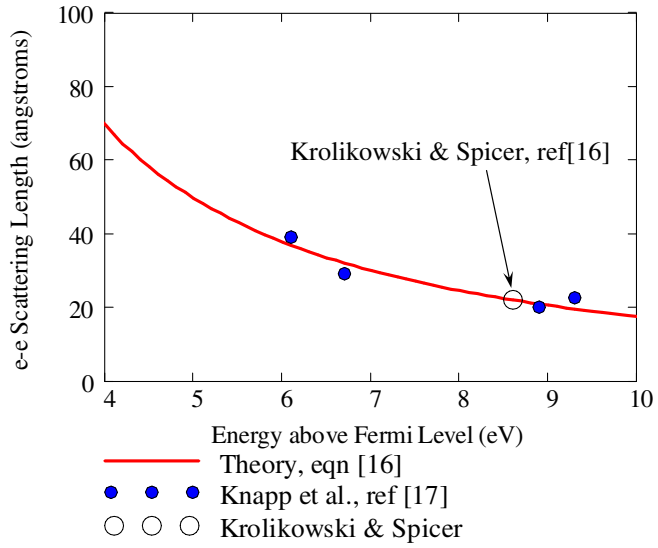

FIG. 7. (Color) The electron-electron scattering length for copper, plotted as a function of electron energy above the Fermi level in the energy range of interest. The length is computed using a Fermi gas model at $T = 0$ as given by Eq. (16) which has been normalized to $\lambda_{\text{e-e}}(E_m = 8.6\text{ eV}) = 22$ Å indicated by the open circle [16]. Measurements in this energy range are plotted as solid circles [19].

for the e-e scattering length is only valid for electron energies near the Fermi level. Above $E' \sim 50$ eV the scattering length increases with energy [18,19].

Since the excited electrons have energies between ϕ_{eff} and $\hbar\omega$ relative to the Fermi level, we evaluate $F_{\text{e-e}}$ at the average electron-electron scattering length,

$$\bar{\lambda}_{\text{e-e}}(\hbar\omega) = \frac{\int_{\phi_{\text{eff}}}^{\hbar\omega} \lambda_{\text{e-e}}(E)dE}{\int_{\phi_{\text{eff}}}^{\hbar\omega} dE} = \frac{2\lambda_m E_m^{3/2}}{\hbar\omega\sqrt{\phi_{\text{eff}}}} \frac{1}{(1 + \sqrt{\frac{\phi_{\text{eff}}}{\hbar\omega}})}. \quad (18)$$

Thus, our final expression for the QE becomes

$$QE(\omega) = \frac{1 - R(\omega)}{1 + \frac{\lambda_{\text{opt}}}{2\lambda_{\text{e-e}}(E_m)} \frac{\hbar\omega\sqrt{\phi_{\text{eff}}}}{E_m^{3/2}} (1 + \sqrt{\frac{\phi_{\text{eff}}}{\hbar\omega}})} \frac{(E_F + \hbar\omega)}{2\hbar\omega} \times \left[1 + \frac{E_F + \phi_{\text{eff}}}{E_F + \hbar\omega} - 2\sqrt{\frac{E_F + \phi_{\text{eff}}}{E_F + \hbar\omega}}\right]. \quad (19)$$

IV. COMPARISON OF THEORY WITH EXPERIMENT

The comparison of theory with the experimental results for the 10.32 mC H-ion data is given in Fig. 8. The theory QE curves are plotted for zero applied electric field, $\phi_{\text{Schottky}} = 0$, corresponding to the field where the QE measurements were performed , and for 50 MV/m as is usually obtained in an rf gun operating with a peak electric field of 100 MV/m and a launch phase of 30° relative to

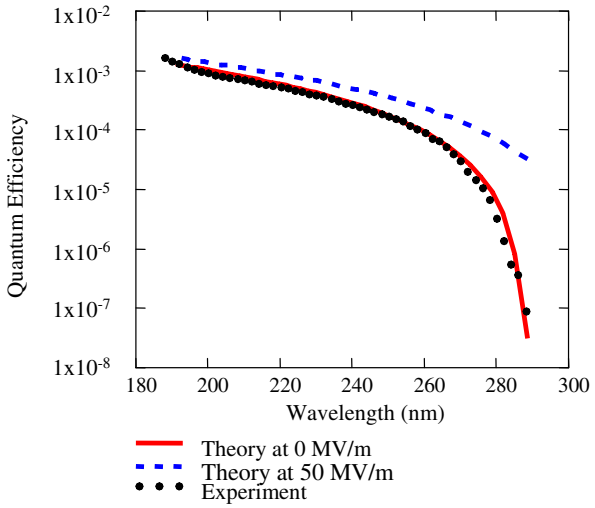

FIG. 8. (Color) Plot comparing the measured QE at low field (points) and computed QE's using Eq. (19) and the parameters listed in Table I at low (red) and high (blue) applied fields.

the zero crossing rf phase. For 50 MV/m, $\phi_{\text{Schottky}} = 0.268$ eV. In this calculation the optical depth and the optical reflectivity are determined from the wavelength-dependent complex index of refraction [20] in Eq. (19) to obtain the theoretical curves shown. The agreement is excellent for the entire wavelength range. Therefore, we conclude the above described theory is reasonably accurate and the H-ion cleaning technique produces a nearly ideal, atomically clean copper surface.

V. IMPLEMENTING THE H-ION CLEANER ON AN *S*-BAND rf GUN

Figure 9 shows a possible method for implementing an H-ion gun on existing 1.6 cell, s-band (2.856 GHz) guns. The H-ion gun working distance is limited to approximately 15 cm, thus transporting the beam through the solenoid is not possible. However, since nearly all such guns are built with grazing-incidence laser ports on the cathode cell, we propose using one of these ports for directing the H-ion beam onto the cathode. The vacuum pressure increases to the 10^{-4} Torr range during H-ion beam operation and, thus, a valve (not shown) is required downstream of the gun and solenoid to protect the rest of the beam line. Work is in progress to investigate installing this type of cleaner on the Linac Coherent Light Source (LCLS) gun. Further details of the LCLS gun can be found in Ref. [21].

TABLE I. Parameters used to compute the theory curves in Fig. 8.

Fermi energy	7 eV
Work function	4.31 eV
ϕ_{Schottky} at 50 MV/m	0.268 eV
e-e scattering length at 8.6 eV	22 Å

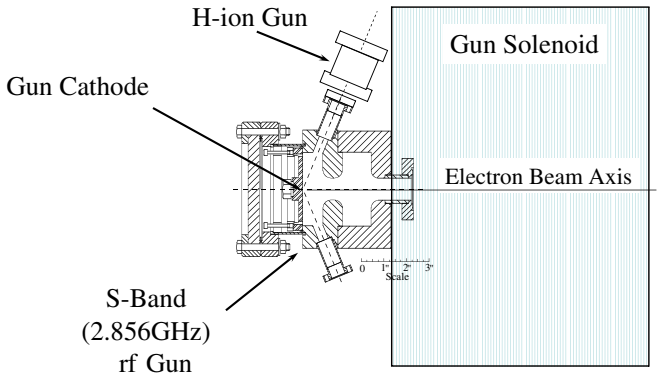

FIG. 9. (Color) The proposed configuration for *in situ* cleaning of the cathode in an s-band rf gun. An H-ion gun with a valve and extension vacuum spool is shown attached to one of the grazing-incidence laser ports on the cathode cell.

VI. SUMMARY AND CONCLUSIONS

This work demonstrates the potential of using a 1 keV hydrogen ion beam to clean the surface of metal cathodes. Measurements of the QE as a function of optical wavelength were performed as a function of the integrated exposures of a copper sample to the hydrogen beam. The QE reached its maximum value after an exposure of 10.32 mC in an area approximately 1 cm in diameter. Analysis of the data yielded a work function of 4.31 eV, slightly lower than but within the experimental uncertainty of the published work function for copper.

In order to understand the fundamental contributions to the QE, a free-electron Fermi gas model was used to derive a relation for the QE. The derivation was based upon the three-step model of photoemission and produces results in exceptional agreement with the measurements. This is due in part to using the experimentally determined work function and the lack of features in the electron density of states of copper near the Fermi level. The results of these studies show that H-ion beam cleaned metal cathodes perform close to the theoretical expectations of an atomically clean metal surface.

Based upon this work, it is proposed to install an H-ion gun on the standard s-band rf gun for *in situ* cleaning of the cathode after its installation. A natural location is one of the laser ports located on the cathode cell of most s-band guns. With the H-ion gun permanently mounted in this location, the cathode can be cleaned whenever it becomes contaminated and the QE is unacceptably low.

ACKNOWLEDGMENTS

SLAC is operated by Stanford University for the Department of Energy under Contract No. DE-AC03-76SF00515. J. Smedley is supported by the Department of Energy Contract No. DE-AC02-98CH10886.

[1] D. Palmer *et al.*, SLAC-PUB-113551.
[2] Atomtech Ltd. Microbeam-7, formerly IonTech, Ltd.
[3] Labview Corp.
[4] R. H. Fowler, Phys. Rev. **38**, 45 (1931).
[5] A. H. Sommer, *Photoemissive Materials, Preparation, Properties and Uses* (John Wiley & Sons, Inc., New York, 1968), pp. 21–26.
[6] *Handbook of Tables for Applied Engineering Science*, edited by R. E. Bolz and G. L. Tuve (CRC Press, Boca Raton, FL, 1986), 2nd ed., p. 317.
[7] *CRC Handbook of Chemistry and Physics, 67th Edition* (CRC Press, Boca Raton, FL, 1986), p. 89.
[8] M. Cardona and L. Ley, *Photoemission in Solids I* (Springer-Verlag, Berlin, 1978), p. 38.
[9] J. F. Schmerge *et al.*, in Proceedings of the 2004 FEL Conference, pp. 205–208. This reference gives a different expression for the QE which is valid for $\hbar\omega > E_F$. The QE given in Eq. (8) is correct for wavelengths corresponding to $\hbar\omega < E_F$, which is the case for the present paper's data and discussion.
[10] C. N. Berglund and W. E. Spicer, Phys. Rev. **136**, A1030 (1964).
[11] M. Cardona and L. Ley, *ibid.*, pp. 22–23.
[12] J. M. Smedley, Ph.D. thesis, State University of New York at Stony Brook, 2001, pp. 50–52, and references contained therein.
[13] A. H. Sommer, *ibid.*, p. 5.
[14] *Handbook of Mathematical Functions with Formulas, Graphs and Mathematical Tables*, edited by M. Abramowitz and I. A. Stegan (Dover, New York, 1972), 9th printing.
[15] K. Gottfried, *Quantum Mechanics* (W.A. Benjamin, Inc., New York, 1966), pp. 443–444.
[16] W. F. Krolikowski and W. E. Spicer, Phys. Rev. **185**, 882 (1969).
[17] J. A. Knapp *et al.*, Phys. Rev. B **19**, 4952 (1979).
[18] D. R. Penn, Phys. Rev. **35**, 482 (1987).
[19] S. Tanuma *et al.*, Surf. Interface Anal. **17**, 911 (1991).
[20] http://www.sopra-sa.com/more/database.asp
[21] For details of the LCLS gun design, see C. Limborg-Deprey *et al.*, Proceedings of the 2005 Particle Accelerator Conference, Knoxville, TN, p. 2233; L. Xiao *et al.*, *ibid.*, p. 3432.